

Supporting Information

Dielectric Environment-Robust Ultrafast Charge Transfer Between Two Atomic Layers

Hongzhi Zhou, Yida Zhao, Haiming Zhu*

Centre for Chemistry of High-Performance & Novel Materials, Department of Chemistry, Zhejiang University, Hangzhou, Zhejiang, 310027, China;

* Email: hmzhu@zju.edu.cn

S1. Experiment details

S2. Comparison between photoexcited TR spectrum and electron doping induced reflectance change

S3. Color plot of TR spectra of WSe₂/WS₂ vdW heterostructures capped with BN and Mica layers

S4. Detailed properties of solvents and dielectrics in this study

S5. ET in WS₂/WSe₂ on SiO₂ substrate in different solvents

S6. Calculation of exciton binding energy in different dielectrics and solvents

S7. ET rate in different solvents assuming nonadiabatic charge transfer process

S8. TR spectra of WSe₂/WS₂ at different temperatures

S1. Experiment details

Sample fabrication. Monolayers of WS₂ and WSe₂ were mechanically exfoliated onto gel-films and SiO₂ (or SiO₂/Si) substrates from bulk crystals (hq graphene). Both monolayers were confirmed by their PL spectra and optical contrast. We fabricated WSe₂/WS₂ heterostructures by dry pick-up and stacking methods.¹⁻² The samples were annealed for 2 hours at 250 °C in high vacuum before measurements. Gated samples were prepared on SiO₂/Si substrate with pre-patterned electrodes and the back-gate voltage was supplied by Keithley 2614b.

Steady-state Optical measurements. The reflectance contrast was measured with a tungsten halogen source (SL201L Thorlabs) by normalizing the reflected spectra from the sample on substrate to that from the bare substrate. The reflected light was collected and analyzed by EMCCD (Princeton Instruments). Photoluminescence spectra was obtained by the same set-up with a 532 nm laser excitation.

Transient reflectance measurements. For time-resolved reflectance measurements, the fundamental beam produced by Yb:KGW laser (Pharos, Light Conversion Ltd) was divided into several light beams. One was introduced to a noncollinear optical parametric amplifier to generate a certain wavelength as pump beam (< 35 fs). The other was focused onto a YAG crystal to generate a continuum white light as probe beam. Both beams were combined and focused by a microscope with a 70 X reflective objective to spots size < 1 μm. (mFemto-TR100, time-tech spectra) The delay time between pump and probe was controlled by a high-resolution motorized delay stage (Newport). The reflected probe light was collected by EMCCD (Princeton Instruments) with the pump beam filtered and the transient reflectance signal was calculated by normalizing the probe spectra from pumped ones to that from unpumped ones. We avoid using transmissive optics along the optical pass and carefully compressed the pump pulse and characterized the pulse duration by FROG. The pump-probe cross-correlation function was performed on a WS₂ monolayer sample under exactly same experiment setup which yields a full-width-at-half-maximum (FWHM) of the convolution of two pulses of < 60 fs (IRF). Therefore, through convolution fitting with a single exponential function, we can accurately extract an ET lifetime > 15 fs (~ IRF/4), as can be justified by the fitting error. Therefore, the ET lifetimes we reported in manuscript are not limited by limited time resolution. Low-temperature measurements were conducted in a microscope cryostat (MicrostatN Oxford Instruments) with sample in high vacuum.

S2. Comparison between photoexcited TR spectrum and electron doping induced reflectance change

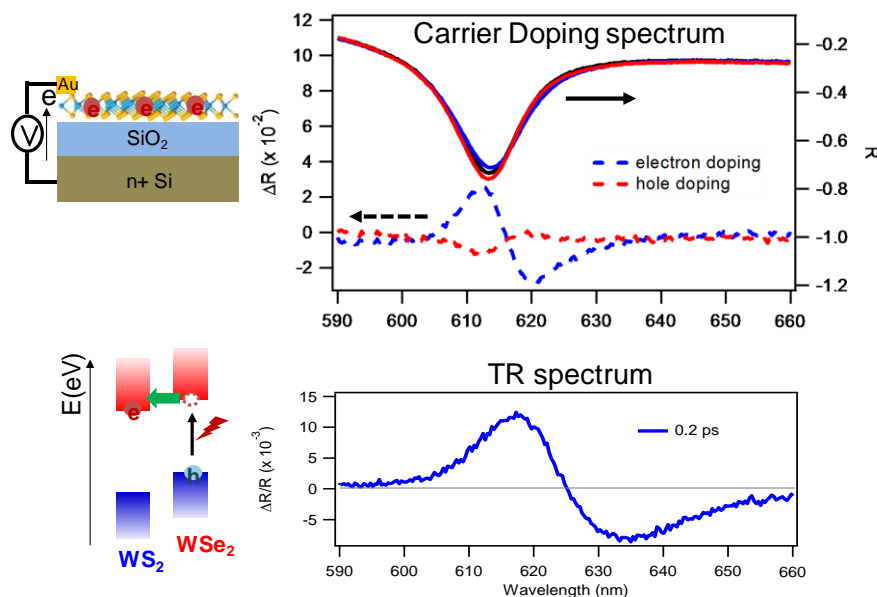


Figure S1. Carrier doping induced reflectance change in WS₂ (top panel) and transient reflectance (bottom panel) on WSe₂/WS₂ heterostructure. The samples were fabricated on SiO₂/Si substrate for applying gating voltage. The agreement between TR spectrum of WSe₂/WS₂ heterostructure and reflectance change of WS₂ under electron doping confirms electron transfer from WSe₂ to WS₂ under WSe₂ excitation. Note the samples here are all on SiO₂ (100nm)/Si substrate for applying back gating therefore the TR spectrum looks different from that on transparent SiO₂, as shown in main text. This doesn't affect the comparison here.

S3. Color plot of TR spectra of WSe₂/WS₂ vdW heterostructures capped with BN and Mica layers

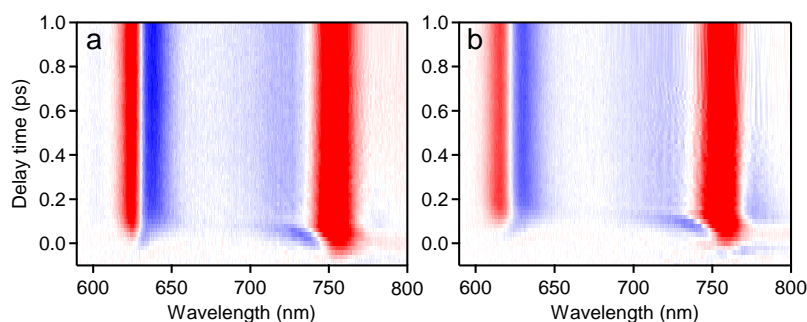


Figure S2. Color plot of TR spectra of WSe₂/WS₂ vdW heterostructures capped with (a) BN and (b) Mica layers. Note the samples here are on SiO₂ (100nm)/Si substrate.

S4. Detailed properties of solvents and dielectrics in this study

Table S1. Properties of different solvents and dielectrics

Solvent	ϵ_{op}	ϵ_{st}	τ_s (ps) ^a	λ (meV) ^b	E_b (meV) ^c
vacuum	1	1		$< 1^d$	306
Toluene	2.3	2.4	1.1	51	259
Chloroform	2.1	4.8	2.3	556	202
Pentanol	2.0	13.9	87	886	107
Isopropanol	1.9	19.9	18	983	79
Ethanol	1.9	24.3	10	1023	66
Methanol	1.8	33.6	2.3	1102	47
Water	1.8	80.4	0.2	1131	17
Formamide	2.1	101.0	0.8	962	13
BN		5			195
Mica		8			150

^a Solvent relaxation time is mostly taken from reference³ and cross-checked with references.⁴⁻⁵ We take 1/e characteristic time $\tau_{1/e}$ as solvent relaxation time and the initial time constant τ_0 is shorter than $\tau_{1/e}$ in a few solvents but still much slower than ET time in vdW heterostructure.

^b Solvent reorganization energy was estimated by $\lambda = \lambda_s/2 = \frac{1}{2} \frac{e^2}{4\pi\epsilon_0 R} \left(\frac{1}{\epsilon_{op}} - \frac{1}{\epsilon_{st}} \right)$,

where $\frac{1}{2}$ considers only half of space filled with solvent, R is half of the monolayer thickness (0.7 nm)

^c The estimate of E_b is shown in details in S6.

^d The reorganization energy of TMD is expected to be very small considering partial compensation of electron-hole pair and their orbital nature.⁶

S5. ET in WS₂/WSe₂ on SiO₂ substrate in different solvents

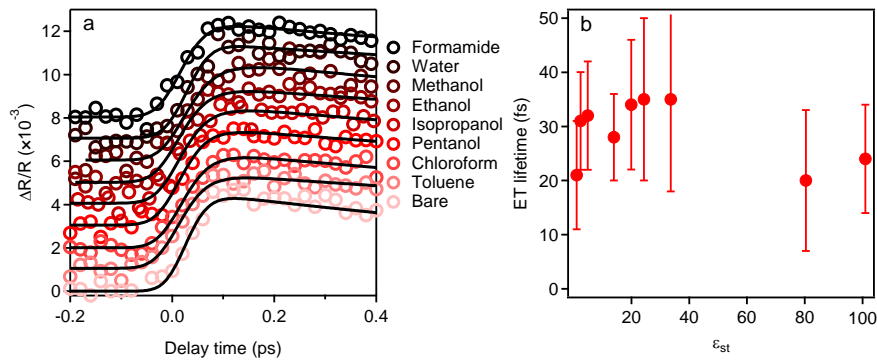


Figure S3. (a) TR kinetics of WS₂/WSe₂ heterostructure (WS₂ on top) immersed in different solvents. ϵ_{st} increases from bottom to top: bare, toluene, chloroform, pentanol, isopropanol, ethanol, methanol, water, formamide. Solid lines are fits to the kinetics. (b) Interfacial ET time in solvents with different ϵ_{st} , showing no dependence on ϵ_{st} .

S6. Calculation of exciton binding energy in different dielectrics and solvents

We consider the potential of exciton in 2D material between substrate and different dielectric environment is strongly dependent on a new variable $\frac{\epsilon_r - \epsilon'}{\epsilon_r + \epsilon'}$, which describe the effect of dielectric field to exciton. ϵ' is dielectric field's relative dielectric constant and ϵ_r is the dielectric constant of TMDs.

we consider the potential experienced by an electron at (ρ, z) due to the presence of a hole at $(0, z_0)$ as:⁷

$$V(\rho) = -\frac{e^2}{4\pi\epsilon_0\epsilon_r} \left\{ \frac{1}{\sqrt{(z-z_0)^2 + \rho^2}} + \frac{\epsilon_r - \epsilon'}{\epsilon_r + \epsilon'} \left[\sum_{n=0}^{\infty} \frac{\left(\frac{\epsilon_r - \epsilon'}{\epsilon_r + \epsilon'}\right)^{2n}}{\sqrt{(z-z_0-2a+2nc)^2 + \rho^2}} \right. \right. \\ \left. \left. + \sum_{n=0}^{\infty} \frac{\left(\frac{\epsilon_r - \epsilon'}{\epsilon_r + \epsilon'}\right)^{2n}}{\sqrt{(z-z_0+2b+2nc)^2 + \rho^2}} \right] + 2\left(\frac{\epsilon_r - \epsilon'}{\epsilon_r + \epsilon'}\right)^2 \sum_{n=0}^{\infty} \frac{\left(\frac{\epsilon_r - \epsilon'}{\epsilon_r + \epsilon'}\right)^{2n}}{\sqrt{(z-z_0+2c+2nc)^2 + \rho^2}} \right\}$$

Since the monolayer we built is 2×10^{-7} m size square on x-y plane and 0.72 nm in height, we make original point at the center of monolayer. $a = -0.36$ nm, $b = 0.36$ nm, is the z coordinate of the lower and upper surface, $c=b-a$ is the thickness of monolayer. $\rho=(x^2+y^2)^{1/2}$ is the distance of electron and hole on x-y plane. We assume $z_0=z$ which means hole and electron are at the same position on z axis. Potential compose of second-order polynomial expansion of independent variable, whose expansion coefficient is the sum of z-direction space finite element contribution. For our model, absolute value of a and b is equal, so we can simply consider $\epsilon' = \frac{\epsilon_{\text{substrate}} + \epsilon_{\text{environment}}}{2}$. We use COMSOL Multiphysics calculate Schrödinger equation of WSe₂ monolayer on SiO₂ under different dielectric environment.

$$\left[-\frac{\hbar^2}{2m_u^*} \nabla^2 + V(\rho) \right] \phi = \lambda \phi$$

the effective mass of the excitonic quasi particle m_u^* can be obtained from

$$\frac{1}{m_u^*} = \frac{1}{m_e^*} + \frac{1}{m_h^*}. \text{ The calculated binding energies are shown in Table 1.}$$

S7. ET rate in different solvents assuming nonadiabatic charge transfer process

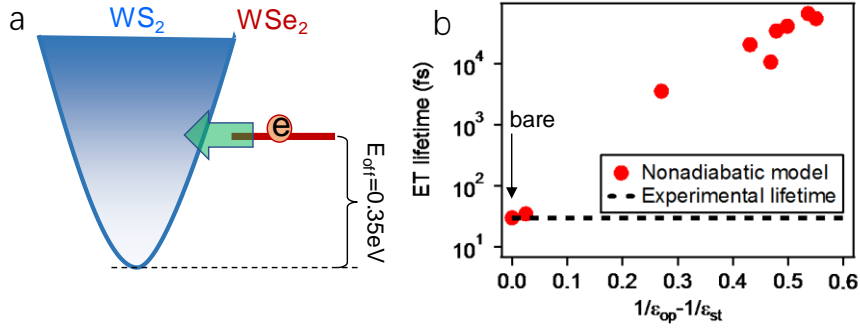


Figure S4. (a) Schematic showing the electron transfer from the conduction band edge in WSe₂ to continuum accepting states in conduction band of WS₂. The quasi-particle band offset is about 0.35 eV. (b) Calculated ET lifetime for different solvents assuming nonadiabatic Marcus ET model involving solvent reorganization. The lifetime of bare sample has been scaled to match the experimental lifetime (~ 30 fs).

We modeled ET process from WSe₂ conduction band to WS₂ conduction band using conventional nonadiabatic Marcus ET model where a single donating state weakly coupled to a continuum accepting states. This model has been extensively applied to describe ET from a molecule or a quantum dot to semiconductor film:⁸⁻⁹

$$k_{ET} = \frac{2\pi}{\hbar} \int_{-\infty}^{\infty} dE \rho(E) |H_{DA}(E)|^2 \frac{1}{\sqrt{4\pi\lambda k_b T}} \exp\left(-\frac{(\lambda + \Delta G_0 + E)^2}{4\lambda k_b T}\right)$$

where $\rho(E)$ is the density of continuum accepting states and can be usually described

by a \sqrt{E} dependence; $|H_{DA}(E)|$ is the electronic coupling which can be assumed to be energy-independent in a small energy range; λ is the reorganization energy including TMDs materials and solvents, the former one is very small (< 1 meV, see Table S1) and we estimated the latter one using simple dielectric continuum model (as shown in Table S1); ΔG_0 is the maximum driving force which is the conduction band offset, which is partially cancelled by intralayer energy binding energy in initial state ($\Delta G_0 = -E_{off} + E_B$). Here we neglect the binding energy in final state (interlayer exciton binding state) since it would be much smaller than the binding energy in initial state⁷ and recent experiment even suggests hot charge transfer state with even smaller binding energy¹⁰. Therefore, the ET rate can be simplified to

$$k_{ET} \propto \int_0^{\infty} dE \sqrt{\frac{E}{\lambda}} \exp\left(-\frac{(\lambda - E_{off} + E_b + E)^2}{4\lambda k_b T}\right)$$

with $E_{off} = 350$ meV, λ and E_b estimated in table S1. We can estimate the relative ET rate in different solvents and the ET rates are shown in Figure S4b as a function of $1/\epsilon_{op} - 1/\epsilon_{st}$ (i.e. reorganization energy). The calculated ET lifetime varies

dramatically in different solvents, contradicting with experimental results.

S8. TR spectra of WSe₂/WS₂ at different temperatures

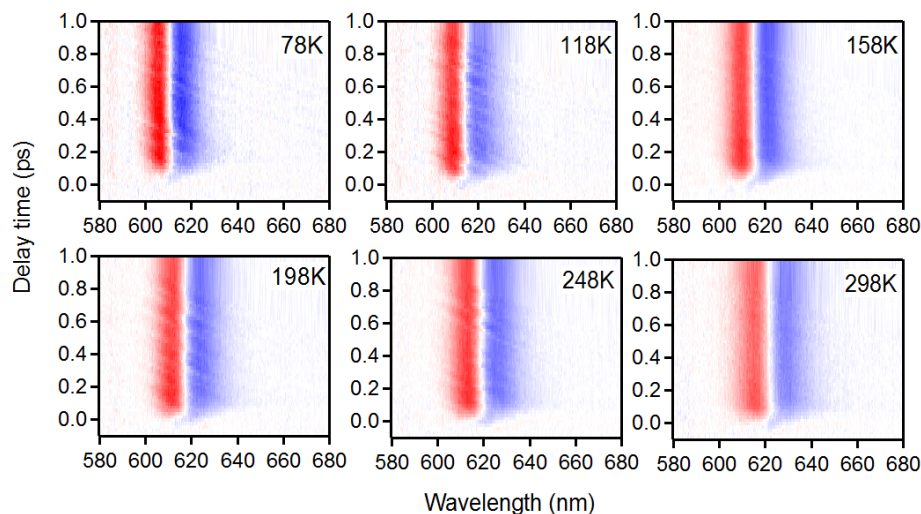


Figure S5. Color plot of TR spectra of WSe₂/WS₂ heterostructure at different temperatures.

References

- Andres, C.-G.; Michele, B.; Rianda, M.; Vibhor, S.; Laurens, J.; Herre, S. J. v. d. Z.; Gary, A. S., Deterministic transfer of two-dimensional materials by all-dry viscoelastic stamping. *2D Materials* **2014**, *1* (1), 011002.
- Zomer, P. J.; Guimarães, M. H. D.; Brant, J. C.; Tombros, N.; Wees, B. J. v., Fast pick up technique for high quality heterostructures of bilayer graphene and hexagonal boron nitride. *Applied Physics Letters* **2014**, *105* (1), 013101.
- Horng, M. L.; Gardecki, J. A.; Papazyan, A.; Maroncelli, M., Subpicosecond Measurements of Polar Solvation Dynamics: Coumarin 153 Revisited. *The Journal of Physical Chemistry* **1995**, *99* (48), 17311-17337.
- Heitele, H., Dynamic Solvent Effects on Electron-Transfer Reactions. *Angew Chem Int Edit* **1993**, *32* (3), 359-377.
- MARONCELLI, M.; MACINNIS, J.; FLEMING, G. R., Polar Solvent Dynamics and Electron-Transfer Reactions. *Science* **1989**, *243* (4899), 1674-1681.
- Parsapour, F.; Kelley, D. F.; Craft, S.; Wilcoxon, J. P., Electron transfer dynamics in MoS₂ nanoclusters: Normal and inverted behavior. *The Journal of Chemical Physics* **1996**, *104* (13), 4978-4987.
- Zhu, X.; Monahan, N. R.; Gong, Z.; Zhu, H.; Williams, K. W.; Nelson, C. A., Charge Transfer Excitons at van der Waals Interfaces. *J Am Chem Soc* **2015**, *137* (26), 8313-20.
- Tvrđy, K.; Frantsuzov, P. A.; Kamat, P. V., Photoinduced electron transfer from semiconductor quantum dots to metal oxide nanoparticles. *Proc. Natl. Acad. Sci.* **2011**, *108* (1), 29-34.
- Anderson, N. A.; Lian, T. Q., Ultrafast electron transfer at the molecule-semiconductor nanoparticle interface. *Annu. Rev. Phys. Chem.* **2005**, *56*, 491-519.

10. Chen, H.; Wen, X.; Zhang, J.; Wu, T.; Gong, Y.; Zhang, X.; Yuan, J.; Yi, C.; Lou, J.; Ajayan, P. M.; Zhuang, W.; Zhang, G.; Zheng, J., Ultrafast formation of interlayer hot excitons in atomically thin MoS₂/WS₂ heterostructures. *Nat Commun* **2016**, 7, 12512.